



# CELLULAR NEURAL NETWORKS: SPACE-DEPENDENT TEMPLATE, MOSAIC PATTERNS AND SPATIAL CHAOS

JONQ JUANG\* and SHIH-FENG SHIEH†

*Department of Applied Mathematics,  
National Chiao Tung University, Hsinchu, Taiwan*

\**jjuang@math.nctu.edu.tw*

†*ssf@math.nctu.edu.tw*

LARRY TURYN

*Department of Mathematics and Statistics,  
Wright State University, Dayton, OH, USA*

*larry.turyn@wright.edu*

Received September 29, 2000; Revised August 9, 2001

We consider a Cellular Neural Network (CNN) with a bias term in the integer lattice  $\mathbb{Z}^2$  on the plane  $\mathbb{Z}^2$ . We impose a space-dependent coupling (template) appropriate for CNN in the hexagonal lattice on  $\mathbb{Z}^2$ . Stable mosaic patterns of such CNN are completely characterized. The spatial entropy of a  $(p_1, p_2)$ -translation invariant set is proved to be well-defined and exists. Using such a theorem, we are also able to address the complexities of resulting mosaic patterns.

*Keywords:* Cellular Neural Networks; space-dependent template; spatial chaos.

## 1. Introduction

The Cellular Neural Networks (CNNs) was originally formulated by Chua and Yang in [1988a, 1988b]. The CNNs without input terms are of the form

$$\begin{aligned} \frac{dx_{i,j}}{dt} &= -x_{i,j} + z \\ &+ \sum_{|k| \leq d, |\ell| \leq d} a_{k,\ell;i,j} f(x_{i+k,i+\ell}), \\ &(i, j) \in \mathbb{Z}^2, \end{aligned} \quad (1a)$$

$$x_{i,j}(0) = x_{i,j}^0. \quad (1b)$$

Here  $x_{i,j}$  denote the state of a cell  $C_{i,j}$ , and  $z$  is an independent voltage source. When  $z = 0$ , (1) is called unbiased; when  $z \neq 0$  it is called biased. The nonlinearity of  $f$  is a piecewise-linear function of the form

$$f(x) = \frac{1}{2} (|x+1| - |x-1|). \quad (2)$$

For fixed  $i, j$ , the numbers  $a_{k,\ell;i,j}|k|, |\ell| \leq d$ ,  $k, \ell \in \mathbb{Z}$  and  $d$  a positive integer, denote the (local) interaction weights between the center cell  $C_{i,j}$  and its neighboring cells  $C_{k,\ell}$ . The numbers  $a_{i,j;k,\ell}, |k| \leq d, |\ell| \leq d$ , can be arranged in a  $(2d+1) \times (2d+1)$  matrix form, which is called a space-dependent

\*Visiting Department of Mathematics, Texas A&M University, College Station, TX and Department of Mathematics and Statistics, Wright State University, Dayton, OH, USA. E-mail: jjuang@math.tamu.edu

$A^{i,j}$ -template

$$A^{i,j} = \begin{bmatrix} a_{i,j;-d,d} & a_{i,j;-d+1,d} & \cdots & a_{i,j;d,d} \\ a_{i,j;-d,d-1} & a_{i,j;-d+1,d-1} & \cdots & a_{i,j;d,d-1} \\ \vdots & \vdots & \vdots & \vdots \\ a_{i,j;-d,-d} & a_{i,j;-d+1,-d} & \cdots & a_{i,j;d,-d} \end{bmatrix}_{(2d+1) \times (2d+1)} \tag{3}$$

$A^{i,j}$  is called space-invariant if  $A^{i,j} \equiv A$  for all  $i, j \in \mathbb{Z}^2$ . If, for each  $i, j, a_{i,j;k,\ell} = a_{i+k,j+\ell;-k,-\ell}$  for all  $|k|, |\ell| \leq d$ , then  $A^{i,j}$  are called symmetric. For further physical and mathematical backgrounds of CNNs as well as their applications, we refer to [Chua, 1998; Chua & Roska, 1993; Chua & Yang, 1988a, 1988b; Crouse *et al.*, 1996; Thiran, 1997, Thiran *et al.*, 1997; Special Issue, 1995]. Much of the theoretical work concerning CNNs focus on the space invariant template. Our motivation for studying a space-dependent template is two-fold. First, chaotic dynamics is only reported (see e.g. [Yen, 1998; Zou *et al.*, 1993; Zou & Nossek, 1991] in case that the template is space-dependent. It seems to be very unlikely that a space-invariant template would yield chaotic dynamics. Second, suppose one considers the regular hexagonal lattice in  $\mathbb{R}^2$  and that each cell, lying on the vertices of hexagons, only directly interacts with its nearest neighbors. Such a problem is equivalent to placing each cell on the integer lattice in  $\mathbb{R}^2$  with a space-dependent template. To see this, consider the following hexagonal lattice in  $\mathbb{R}^2$ .

We assume that each cell only directly interacts with its nearest neighbors. For instance, the cell  $F$  only directly interacts with cells  $E, G$  and  $I$ . Now, if one squeezes each hexagon into a square, we will get the following integer lattice in  $\mathbb{R}^2$

From Fig. 2, we see that the cell  $E$  interacts with the cell  $A$ , which is on top of  $E$ , while the cell

$F$  does not interact with the cell  $B$ . Thus, to study the dynamical systems on hexagonal lattice in  $\mathbb{R}^2$  we consider an equivalent problem on integer lattice in  $\mathbb{R}^2$  with the following space-dependent template  $A^{i,j}$ .

$$A^{i,j} = \begin{bmatrix} 0 & a_{i,j;0,1} & 0 \\ a_{i,j;-1,0} & a_{i,j;0,0} & a_{i,j;1,0} \\ 0 & a_{i,j;0,-1} & 0 \end{bmatrix} = \begin{cases} \begin{bmatrix} 0 & a_3 & 0 \\ a_1 & a & a_2 \\ 0 & 0 & 0 \end{bmatrix} & \text{if } i+j \text{ is even} \\ \begin{bmatrix} 0 & 0 & 0 \\ b_2 & b & b_1 \\ 0 & b_3 & 0 \end{bmatrix} & \text{if } i+j \text{ is odd.} \end{cases} \tag{4}$$

In this paper, we investigate the mosaic patterns of (1), (2), and (4) and the complexity of mosaic patterns. Some simulations of the CNN mosaic patterns are given in the appendix. A mosaic solution  $\bar{x} = (\bar{x}_{i,j})$  is a stationary solution of (1a) satisfying  $|\bar{x}_{i,j}| > 1$  for all  $(i, j) \in \mathbb{Z}^2$  and  $y = (f(\bar{x}_{i,j}))$  is called a mosaic pattern.

Mosaic solutions of lattice dynamical systems have been studied by many authors ([Chow & Mallet-Paret, 1995a, 1995b; Chow *et al.*, 1996a, 1996b] and the work cited therein). In the case of CNNs, mosaic patterns of one-dimensional CNNs with symmetric, space-invariant template,  $[b, a, b]$ , were studied by Thiran [1997] etc. Mosaic patterns

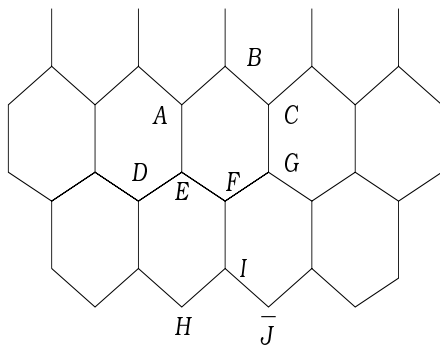


Fig. 1. The hexagonal lattice in  $\mathbb{R}^2$ .

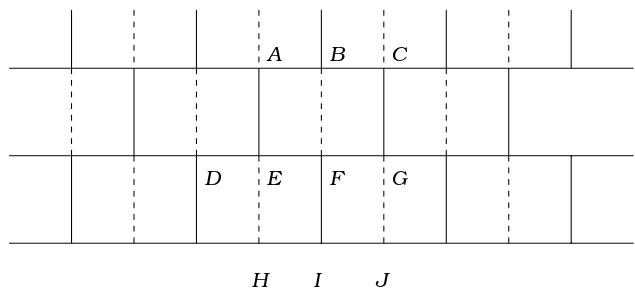


Fig. 2. The integer lattice in  $\mathbb{R}^2$  squeezed from Fig. 1.

of two-dimensional CNNs with symmetric coupling between nearest neighbors, and also next-nearest neighbors are completely characterized by Juang and Lin [2000]. In [Shih, 1998], mosaic patterns of two-dimensional CNNs with asymmetric template were investigated. Local patterns for general space-invariant templates were studied in [Hsu *et al.*, 2000].

## 2. Notations and Preliminaries

Given a template  $A^{i,j}$ , as defined in (3), and a biased term  $z$ , the stationary equation for (1a) is

$$x_{i,j} = z + \sum_{|k| \leq 1, |\ell| \leq 1} a_{k,\ell;i,j} f(x_{i+k,j+\ell}), \quad (i, j) \in \mathbb{Z}^2. \tag{5}$$

Let  $x = (x_{i,j})$  be a solution of (5). Two types of stationary solutions are of interest: mosaic and

defect. A defect solution  $\bar{x} = (\bar{x}_{i,j})$  satisfies  $|\bar{x}_{i,j}| > 1$  for  $(i, j) \in \mathbb{Z}^2 \setminus D$  and  $|\bar{x}_{k,\ell}| < 1$  for  $(k, \ell) \in D$ , where  $D \neq \emptyset$  and  $D \neq \mathbb{Z}^2$ . Its corresponding pattern  $\bar{y} = (f(\bar{x}_{i,j}))$  is called a defect pattern. Let  $x = (x_{i,j})$  be a (defect or mosaic) solution of (5), we denote  $\Gamma_+$ ,  $\Gamma_-$  and  $\Gamma_\times$  as follows

$$\begin{aligned} \Gamma_+ &= \{(i, j) \in \mathbb{Z}^2 : x_{i,j} > 1\} \\ \Gamma_- &= \{(i, j) \in \mathbb{Z}^2 : x_{i,j} < -1\}, \end{aligned} \tag{6a}$$

and

$$\Gamma_\times = \{(i, j) \in \mathbb{Z}^2 : |x_{i,j}| < 1\}, \tag{6b}$$

respectively. Let  $\mathbb{Z}_E^2 = \{(i, j) : i, j \in \mathbb{Z} \text{ and } i + j \text{ is even}\}$  and  $\mathbb{Z}_O^2 = \{(i, j) : i, j \in \mathbb{Z} \text{ and } i + j \text{ is odd}\}$ . If  $(i, j) \in \mathbb{Z}_E^2$  (resp.  $\mathbb{Z}_O^2$ ), then  $(i, j)$  is called even (resp. odd point). Stability is then studied using spectral theory. Let  $\xi = (\xi_{i,j}) \in \ell^2$ , a suitable weighted  $\ell^2$  space. The linearized operator  $\mathcal{L}(x)$  of (5) at  $x$  is given by

$$(\mathcal{L}(x)\xi)_{i,j} = \begin{cases} -\xi_{i,j} + L_{i,j}, & \text{if } (i, j) \in \Gamma_+ \cup \Gamma_-, \\ (a_{i,j;0,0} - 1)\xi_{i,j} + L_{i,j}, & \text{if } (i, j) \in \Gamma_\times. \end{cases} \tag{7a}$$

Here,

$$L_{i,j} = \sum_{(k,\ell) \in N^+(i,j) \in \Gamma_\times} a_{i,j;k,\ell} \xi_{k,\ell} \tag{7b}$$

and

$$N^+(i, j) = \{(p, q) \in \mathbb{Z}^2 : |p - i| + |q - j| = 1\}, \tag{7c}$$

**Definition 2.1.** Let  $x = (x_{i,j})$  be a solution of (5) with  $|x_{i,j}| \neq 1$  for all  $(i, j) \in \mathbb{Z}^2$ .  $x$  is then called (linearized) *stable* if all eigenvalues of  $\mathcal{L}(x)$  have negative real parts. The solution  $x$  is called *unstable* if there is an eigenvalue  $\lambda$  of  $\mathcal{L}(x)$  such that  $\lambda$  has a positive real part.

**Theorem 2.1.** Let  $x = (x_{i,j})$  be a solution of (5) and let the templates  $A^{i,j}$  be given as in (4). Then the following holds. (i) If  $A^{i,j}$  are symmetric for all  $i, j$ , then  $\mathcal{L}(x)$  is self-adjoint. (ii) If  $x$  is a mosaic solution of (5), then  $x$  is stable. (iii) If  $a_{i,j;0,0} > 1$  for all  $(i, j) \in \mathbb{Z}^2$ , and  $x$  is a defect solution, then  $x$  is unstable.

*Remark*

- (1) Theorem 2.1 is a direct generalization of Theorem 2.4 of [Juang & Lin, 2000].
- (2) If  $A^{i,j}$  are given as in (4), then  $A^{i,j}$  are symmetric if and only if  $a_i = b_i$   $i = 1, 2, 3$ .

To study the complexity of mosaic patterns, we review some definitions and results concerning spatial entropy. Let  $\mathcal{A}$  be a finite set of  $d$  elements and  $D \geq 1$  be an integer representing the lattice dimension. Denote by  $\mathcal{A}^{\mathbb{Z}^D}$  the set of all mappings  $y: \mathbb{Z}^D \rightarrow \mathcal{A}$ . In our case,  $D = 2$ ,  $d = 2$  and  $\mathcal{A} = \{-1, 1\}$  for the mosaic patterns. Consider any nonempty subset  $\mathcal{U} \subseteq \mathcal{A}^{\mathbb{Z}^2}$ . Here  $\mathcal{U}$  will represent the mosaic patterns. The set  $\mathcal{U}$  is said to be *translation invariant* if  $S_k(\mathcal{U}) = \mathcal{U}$ ,  $k = 1, 2, \dots, D$ , where  $S_k: \mathcal{A}^{\mathbb{Z}^D} \rightarrow \mathcal{A}^{\mathbb{Z}^D}$  is a shift operator. To save our notation later, we write  $S_k(\mathcal{U}) = \mathcal{U}$  as  $\mathcal{U} + e_k = \mathcal{U}$ . Here  $e_k$  is the unit basis vector in the  $k$ th direction of  $\mathbb{R}^D$ . Let  $\Gamma_N(\mathcal{U})$  count the number of distinct patterns among the elements of  $\mathcal{U}$  restricted in a given rectangle of size  $N_1 \times N_2$ .

**Definition 2.2.** The set  $\mathcal{U}$  is said to be  $(p_1, p_2)$ -translation invariant if there exist non-negative integers  $p_1, p_2$  such that  $\sum_{i=1}^2 p_i \geq 1$  and  $\mathcal{U} + (p_1, 0) = \mathcal{U} + (0, p_2) = \mathcal{U}$ . The *spatial entropy*  $h(\mathcal{U})$  of the set  $\mathcal{U}$  is defined as the limit

$$h(\mathcal{U}) = \lim_{N_1, N_2 \rightarrow \infty} \frac{\log \Gamma_N(\mathcal{U})}{N_1 N_2}, \tag{8}$$

where the limit is taken over *all* possible choices of  $N_1 \times N_2$  rectangles.

In CNNs, if the template is space-invariant, then any stationary solution of (1a) is translation invariant. Note that if the template  $A^{i,j}$  is given as in (4), then any stationary solution of (1a) is (1, 1)-translation invariant. One of our main results, Theorem 4.1, will show that the spatial entropy  $h(\mathcal{U})$  is well-defined and exists provided that  $\mathcal{U}$  is  $(p_1, p_2)$ -translation invariant.

**Definition 2.3.** Let  $\mathcal{U}$  be a translation invariant subset of  $\mathcal{A}^{\mathbb{Z}^D}$ ;  $\mathcal{U}$  exhibits *spatial chaos* if the spatial entropy  $h(\mathcal{U})$  is greater than zero. Otherwise,  $\mathcal{U}$  exhibits *pattern formation*.

### 3. Local Mosaic Patterns

To simplify our representation, we consider the templates given in (4) with  $a = b$ , and  $a_i = b_i$ ,  $i = 1, 2, 3$ . We first set the following notations

$$A^{i,j} = \begin{cases} \begin{bmatrix} 0 & a_1 & 0 \\ a_1 & a & a_1 \\ 0 & 0 & 0 \end{bmatrix} := A_E & \text{if } (i, j) \in \mathbb{Z}_E^2 \\ \begin{bmatrix} 0 & 0 & 0 \\ a_1 & a & a_1 \\ 0 & a_1 & 0 \end{bmatrix} := A_O & \text{if } (i, j) \in \mathbb{Z}_O^2, \end{cases} \tag{9}$$

$$N_E^+(i, j) = \{(p, q) \in \mathbb{Z}^2 : |p - i| + |q - j| = 1, q - j > 0\}, \quad i + j \text{ is even},$$

$$N_O^-(i, j) = \{(p, q) \in \mathbb{Z}^2 : |p - i| + |q - j| = 1, q - j < 0\}, \quad i + j \text{ is odd}.$$

**Definition 3.1.** Given any proper subset  $T \subseteq \mathbb{Z}^2$ ,  $x|_T (\equiv x^T)$  is called a *local mosaic solution* if  $x^T$  is a restriction of some mosaic solution  $x$  of (5) on  $T$ . The restriction  $(f(x_{i,j}))|_T$  on  $T$  is called a *local pattern*, and will be denoted by  $(f(x_{i,j}))|_T = (y_{i,j}^T) = y^T$ ; when  $T = \mathbb{Z}^2$ ,  $y$  is called a *global mosaic pattern*.

**Definition 3.2.** A set  $T \subseteq \mathbb{Z}^2$  is called *basic* with respect to the template  $A^{i,j}$ , as given in (4), if  $T = \{(i, j)\} \cup N_E^+(i, j)$ , where  $i + j$  is even or  $T = \{(i, j)\} \cup N_O^-(i, j)$ , where  $i + j$  is odd. A *basic*

*mosaic pattern* is a local pattern defined on some basic set  $T$ .

**Notation 3.1.** Let  $y^T$  be a local mosaic pattern on a subset  $T \subseteq \mathbb{Z}^2$ . For any  $(i, j) \in T$ , if  $f(x_{i,j}) = 1$  (resp.  $f(x_{i,j}) = -1$ ), then to draw a figure for  $y^T$  the output  $f(x_{i,j})$  of the state of the cell  $C_{i,j}$  will be denoted by  $+$  (resp.  $-$ ).

For any  $(i, j) \in \mathbb{Z}_E^2$ , a basic mosaic pattern  $y^T$  must have one of the following forms.

$$\begin{aligned} \text{(i)} & \quad + \bullet + & \text{(ii)} & \quad - \bullet + & \text{(iii)} & \quad + \bar{\bullet} + & \text{(iv)} & \quad + \bullet - \\ \text{(v)} & \quad - \bar{\bullet} + & \text{(vi)} & \quad - \bullet - & \text{(vii)} & \quad + \bar{\bullet} - & \text{(viii)} & \quad - \bar{\bullet} -. \end{aligned} \tag{10}$$

Here  $\bullet$  is either  $+$  or  $-$ , the output of the state of the (center) cell  $C_{i,j}$ . For any  $(i, j) \in \mathbb{Z}_O^2$ , a basic pattern  $y^T$  also has eight possible forms which are obtained by rotating the forms in (10) by  $180^\circ$ .

**Notation 3.2.** Let  $V_\bullet = \{v_\bullet \in \mathbb{R}^3, v_\bullet = (v_1, v_2, v_3)_\bullet, |v_i| = 1, i = 1, 2, 3\}$ . Here  $\bullet = +$  or  $-$ . Clearly,  $V_\bullet$  can be used to represent all eight possible forms in (10). For instance, we may identify the output of the state of the cells  $C_{i-1,j}, C_{i,j+1}$  (or  $C_{i,j-1}$ ), and  $C_{i+1,j}$  as  $v_1, v_2$ , and  $v_3$ , respectively. With such identification,  $+++ = (1, 1, 1)_+$  and  $+- - = (1, 1, -1)_-$ . We shall use  $V_\bullet^E$  or  $V_\bullet^O$  to distinguish the position of the center cell provided the distinction is needed.

**Definition 3.3.** For any  $(i, j) \in \mathbb{Z}^2$ , the *total output* of any basic mosaic pattern whose center is at  $(i, j)$  is defined to be  $v_1 + v_2 + v_3$ .

We are now in a position to study the local basic mosaic patterns. Let  $(i, j) \in \mathbb{Z}^2$ , the state  $x_{i,j}$  of the cell  $C_{i,j}$  is greater than one if and only if

$$a_1(y_{i-1,j} + y_{i,j+1} + y_{i+1,j}) + a + z - 1 > 0. \tag{11a}$$

Similarly,  $x_{i,j} < -1$  if and only if

$$a_1(y_{i-1,j} + y_{i,j+1} + y_{i+1,j}) - a + z + 1 > 0. \tag{11b}$$

Since  $(y_{i-1,j}, y_{i,j+1}, y_{i+1,j}) \in V_\bullet$ , inequality (3.3) can be, respectively, simplified as follows

$$ka_1 + a + z - 1 > 0, \tag{12a}$$

and

$$ka_1 - a + z + 1 > 0, \tag{12b}$$

where  $k = 3, 1, -1, -3$ .

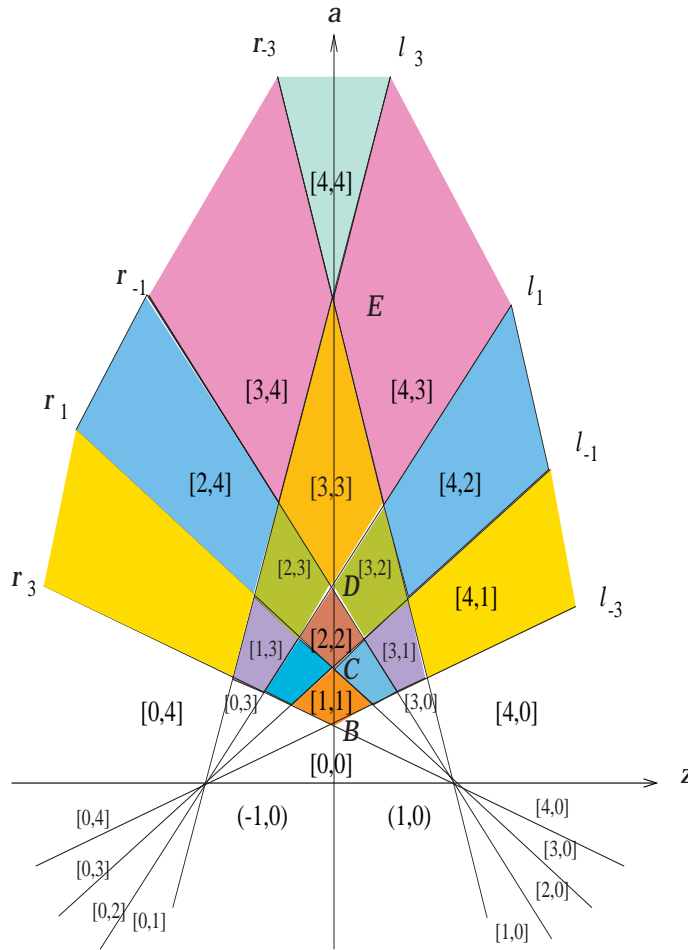


Fig. 3.  $B = 1/1 + 3|\varepsilon|$ ,  $C = 1/1 + |\varepsilon|$ ,  $D = 1/1 - |\varepsilon|$ ,  $E = (1/1 - 3|\varepsilon|)$   $0 < |\varepsilon| < 1/3$ . Here  $[m, n]_\varepsilon = [m, n]$ ,  $\ell_{i,|\varepsilon|} = \ell_i$  and  $r_{i,|\varepsilon|} = r_i$ ,  $i \in \{3, 1, -1, -3\}$ . The classification of parameter space with respect to the mosaic patterns.

If we treat  $a_1$ ,  $a$  and  $z$  as three independent variables, the regions separated by those inequalities in (12) are difficult to picture. To better visualize the regions, we set  $a_1 = a\varepsilon$ . The inequalities (12) then reduce to

$$a(1 + \varepsilon k) + z > 1 \tag{13a}$$

$$a(-1 + \varepsilon k) + z > -1, \quad \text{where } k = 3, 1, -1, -3. \tag{13b}$$

Let  $r_{k,\varepsilon}$  and  $\ell_{k,\varepsilon}$  be straight lines whose equations are, respectively,

$$a(1 + \varepsilon k) + z = 1 \tag{14a}$$

and

$$a(-1 + \varepsilon k) + z = -1. \tag{14b}$$

Let  $\ell$  be a straight line that does not pass through the origin in a plane. Denote by  $\ell(0)$  the

open half-plane containing the origin, while  $\ell(\times)$  denotes the other open half-plane.

For fixed  $0 < |\varepsilon| < 1/3$ , the straight lines in (14) divide  $z - a$  plane into the following disjoint regions.

In Fig. 3, we see, for instance,

$$[4, 4]_\varepsilon = \ell_{3,|\varepsilon|}(\times) \cap r_{-3,|\varepsilon|}(\times),$$

and

$$[2, 2]_\varepsilon = \ell_{-1,|\varepsilon|}(\times) \cap \ell_{1,|\varepsilon|}(0) \cap r_{-1,|\varepsilon|}(0) \cap r_{1,|\varepsilon|}(\times).$$

In general, for  $m, n \in \{1, 2, 3, 4\}$  and  $a > 0$ ,

$$[m, n]_\varepsilon = r_{-2m+5,|\varepsilon|}(\times) \cap r_{-2m+3,|\varepsilon|}(0) \cap \ell_{2n-3,|\varepsilon|}(0) \cap \ell_{2n-5,|\varepsilon|}(\times). \tag{15a}$$

Here, if  $|k| > 3$ , then  $r_{k,|\varepsilon|}(\cdot)$  and  $\ell_{k,|\varepsilon|}(\cdot)$  are interpreted as the  $z - a$  plane  $P_2$ . For  $m, n \in \{1, 2, 3, 4\}$

and  $a < 0$ ,

$$[m, 0]_\varepsilon = r_{2m-3,|\varepsilon|}(0) \cap r_{2m-5,|\varepsilon|}(\times) \cap \ell_{3,|\varepsilon|}(0), \tag{15b}$$

$$[0, n]_\varepsilon = \ell_{5-2n,|\varepsilon|}(\times) \cap \ell_{3-2n,|\varepsilon|}(0) \cap r_{-3,|\varepsilon|}(0), \tag{15c}$$

and

$$[0, 0]_\varepsilon = \ell_{3,|\varepsilon|}(0) \cap r_{-3,|\varepsilon|}(0). \tag{15d}$$

We omit the subscript  $\varepsilon$  where the meaning is clear.

*Remark.* For  $1/3 \leq |\varepsilon| < 1$ , the  $a$ -intercept  $E$  (see Fig. 3) of  $r_{-3,|\varepsilon|}$  and  $\ell_{3,|\varepsilon|}$  lies either below the  $z$ -axis or does not exist. This implies that the region  $[4, 4]$  will disappear. For  $|\varepsilon| \geq 1$ , the regions  $[3, 3]$ ,  $[3, 4]$ , and  $[4, 3]$  will no longer exist.

**Theorem 3.1.** *Let  $0 < |\varepsilon| < 1/3$ , and  $[m, n]_\varepsilon$  be the disjoint (open) regions described in (15) and shown in Fig. 3. Suppose  $(z, a) \in [m, n]_\varepsilon$  and  $a\varepsilon > 0$ . Then any basic mosaic pattern in  $V_+$  (resp.  $V_-$ ) whose total output is greater or equal to  $5-2m$  (resp. no greater than  $2n-5$ ) exists. Suppose  $(z, a) \in [m, n]_\varepsilon$  and  $a\varepsilon < 0$ . Then any basic mosaic pattern in  $V_+$  (resp.  $V_-$ ) whose total output is no greater than  $2m-5$  (resp. no less than  $5-2n$ ) exists.*

*Proof.* We illustrate only for  $[3, 3]_\varepsilon$  and  $a\varepsilon > 0$ . The illustration for other regions can be similarly derived. Note that  $[3, 3]_\varepsilon$  is bounded by  $\ell_{1,|\varepsilon|}$ ,  $\ell_{3,|\varepsilon|}$ ,  $r_{-3,|\varepsilon|}$  and  $r_{-1,|\varepsilon|}$ . If  $(z, a) \in r_{-1,|\varepsilon|}(\times) \cap r_{-3,|\varepsilon|}(0)$ ,  $a > 0$  and  $\varepsilon > 0$ , then any positively saturated cells whose three neighbors are shown in (10) must have at least one positively saturated neighbor. Thus, if  $(z, a) \in r_{3,|\varepsilon|}(0) \cap r_{1,|\varepsilon|}(\times)$ ,  $a > 0$  and  $\varepsilon > 0$ , then the total output of any basic mosaic pattern in  $V_+$  is no less than  $-1$ . Moreover, if  $(z, a) \in \ell_{3,|\varepsilon|}(0) \cap \ell_{1,|\varepsilon|}(\times)$ ,  $a > 0$  and  $\varepsilon > 0$ , then the total output of any mosaic pattern in  $V_-$  is no greater than 1. ■

*Remark.* Suppose  $(z, a) \in [m, n]$ , where  $a\varepsilon > 0$ . Then any basic mosaic pattern in  $V_+$  (resp.  $V_-$ ) exists provided that the center of the pattern must be coupled to at least  $(4-m)+$ 's (resp.  $(4-n)-$ 's). See (10). Suppose  $(z, a) \in [m, n]$  and  $a\varepsilon < 0$ . Then any basic mosaic pattern in  $V_+$  (resp.  $V_-$ ) exists provided that the center of the pattern must be coupled to at least  $(4-m)-$ 's (resp.  $(4-n)+$ 's).

Denote by  $\mathcal{F}_E([m, n])$  (resp.  $\mathcal{F}_O([m, n])$ ) the set of all basic mosaic patterns that have parameter  $\varepsilon$  in  $[m, n]$  and is centered at  $(i, j)$ , where  $(i, j) \in \mathbb{Z}_E^2$  (resp.  $\mathbb{Z}_O^2$ ).

**Corollary 3.1.** *Suppose  $a\varepsilon > 0$ , and let  $\bullet$  be either + or -. Then*

- (i)  $\mathcal{F}_E([4, 4]) = \left\{ \begin{matrix} \bullet & \bullet & \bullet \\ \bullet & + & \bullet \\ \bullet & \bullet & \bullet \end{matrix} , \begin{matrix} \bullet & \bullet & \bullet \\ \bullet & - & \bullet \\ \bullet & \bullet & \bullet \end{matrix} \right\}$ ;  $\mathcal{F}_O([4, 4]) = \left\{ \begin{matrix} \bullet & + & \bullet \\ \bullet & \bullet & \bullet \\ \bullet & \bullet & \bullet \end{matrix} , \begin{matrix} \bullet & - & \bullet \\ \bullet & \bullet & \bullet \\ \bullet & \bullet & \bullet \end{matrix} \right\}$ .
- (ii)  $\mathcal{F}_E([3, 3]) = \left\{ \begin{matrix} \bullet & \bullet & \bullet \\ + & + & \bullet \\ \bullet & \bullet & \bullet \end{matrix} , \begin{matrix} \bullet & \bullet & \bullet \\ + & + & \bullet \\ - & - & \bullet \end{matrix} , \begin{matrix} \bullet & \bullet & \bullet \\ - & - & \bullet \\ \bullet & \bullet & \bullet \end{matrix} , \begin{matrix} \bullet & \bullet & \bullet \\ - & - & \bullet \\ \bullet & \bullet & \bullet \end{matrix} \right\}$ .  $\mathcal{F}_O([3, 3])$  is the rotation of  $\mathcal{F}_E([3, 3])$  by  $180^\circ$ .
- (iii)  $\mathcal{F}_E([2, 2]) = \left\{ \begin{matrix} + & \bullet \\ + & + \end{matrix} , \begin{matrix} \bullet & + \\ + & + \end{matrix} , \begin{matrix} + & - \\ - & - \end{matrix} , \begin{matrix} - & \bullet \\ - & - \end{matrix} , \begin{matrix} - & - \\ \bullet & - \end{matrix} \right\}$ .  $\mathcal{F}_O([2, 2])$  is the rotation of  $\mathcal{F}_E([2, 2])$  by  $180^\circ$ .
- (iv)  $\mathcal{F}_E([1, 1]) = \left\{ \begin{matrix} + \\ + \end{matrix} , \begin{matrix} - \\ - \end{matrix} \right\}$ ;  $\mathcal{F}_O([1, 1]) = \left\{ \begin{matrix} + \\ + \end{matrix} , \begin{matrix} - \\ - \end{matrix} \right\}$ .
- (v)  $\mathcal{F}([0, 0]) = \emptyset$ .

The other cases can be constructed accordingly.

### 4. Global Mosaic Patterns and Their Complexities

To see the complexities of a certain set of global mosaic patterns, we first show that the limit in (8) is well-defined and exists provided that  $\mathcal{U}$  is  $(p_1, p_2)$ -translation invariant. We note that with the templates given as in (4), any stationary solution  $x$  of (1a) is  $(2, 2)$ -translation invariant. To this end, we need the following notation.

**Definition 4.1.** Let  $N = (N_1, N_2)$  be a two-tuple of positive integers, and let  $\Gamma_N^{(i,j)}(\mathcal{U})$  count the number of distinct patterns among the elements of  $\mathcal{U}$  restricted to a rectangle of size  $N_1 \times N_2$  whose lower left corner point is at  $(i, j)$ . When the reasoning is general, we may omit the  $(i, j)$  and write only  $\Gamma_N(\mathcal{U})$ .

**Definition 4.2.** Let  $p_1$  and  $p_2$  be as in Definition 2.2. A standard window  $N$  is a rectangle of size  $N_1 \times N_2$ , where  $N_1$  and  $N_2$  are positive integer

multiples of  $p_1$  and  $p_2$ , respectively, whose lower left corner point is at  $(p_1k_1, p_2k_2)$  for some integers  $k_1, k_2$ .

We note that if  $N$  is any rectangle then there are standard windows  $\tilde{N}$  and  $\hat{N}$  with  $\tilde{N} \subseteq N \subseteq \hat{N}$  and the areas of  $N \setminus \tilde{N}$  and  $\hat{N} \setminus N$  are less than  $\delta := 4(p_1N_2 + p_1N_2)$ . It follows that

$$\Gamma_{\hat{N}}(\mathcal{U}) \leq 2^\delta \Gamma_N(\mathcal{U}) \quad \text{and} \quad \Gamma_N(\mathcal{U}) \leq 2^\delta \Gamma_{\tilde{N}}(\mathcal{U}),$$

because the cardinality of  $\mathcal{A}$  being two implies that there are at most  $2^\delta$  ways to put symbols in the regions  $\hat{N} \setminus N$  or  $N \setminus \tilde{N}$ . So,

$$2^{-\delta} \Gamma_{\tilde{N}}(\mathcal{U}) \leq \Gamma_N(\mathcal{U}) \leq 2^\delta \Gamma_{\hat{N}}(\mathcal{U}). \quad (16)$$

We are now ready to state one of our main results in this section.

**Theorem 4.1.** *Suppose  $\mathcal{U}$  is  $(p_1, p_2)$ -translation invariant. Then the limit in (8) is well-defined and exists.*

*Proof.* First,

$$\lim_{N_1, N_2 \rightarrow \infty} \frac{\log \Gamma_N(\mathcal{U})}{N_1 N_2}$$

exists when the limit is restricted to standard windows  $N$ , using the methods of [Chow *et al.*, 1996, Sec. 5]. Next, let  $N$  be any window and let  $\tilde{N}$  and  $\hat{N}$  be standard windows chosen to get (16). Let the sizes of  $\tilde{N}$  and  $\hat{N}$  be  $\tilde{N}_1 \times \tilde{N}_2$  and  $\hat{N}_1 \times \hat{N}_2$ , respectively. We have

$$\begin{aligned} & \frac{\hat{N}_1 \hat{N}_2}{N_1 N_2} \frac{-\delta \log 2 + \log \Gamma_{\hat{N}}(\mathcal{U})}{\hat{N}_1 \hat{N}_2} \\ & \leq \frac{\log \Gamma_N(\mathcal{U})}{N_1 N_2} \\ & \leq \frac{\tilde{N}_1 \tilde{N}_2}{N_1 N_2} \frac{\delta \log 2 + \log \Gamma_{\tilde{N}}(\mathcal{U})}{\tilde{N}_1 \tilde{N}_2}. \end{aligned}$$

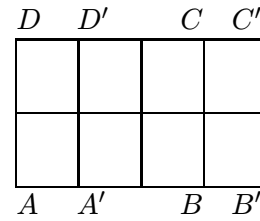
Because  $\delta/N_1 N_2 = 4(p_1 N_2 + p_1 N_2)/N_1 N_2$ , the existence of

$$\lim_{N_1, N_2 \rightarrow \infty} \frac{\log \Gamma_N(\mathcal{U})}{N_1 N_2}$$

follows. ■

We note that with the templates given as in (4), even more is true:  $\Gamma_{(2n+1, 2n)}^{(0,0)}(\mathcal{U}) = \Gamma_{(2n+1, 2n)}^{(1,0)}(\mathcal{U})$  for

all positive integers  $n$ . We illustrate this by considering the following two rectangles,  $ABCD$  and  $A'B'C'D'$ , of size  $2 \times 3$  whose lower left corners are  $A(0, 0)$  and  $A'(1, 0)$ .



Clearly,  $A, D, B'$  and  $C' \in \mathbb{Z}_E^2$  and  $A', D', B$  and  $C \in \mathbb{Z}_O^2$ . By rotating by  $180^\circ$  a pattern restricted on the rectangle  $ABCD$ , we would get a pattern that can be fit in the rectangle  $A'B'C'D'$ . The converse is also true. Hence,

$$\Gamma_{(3,2)}^{(0,0)}(\mathcal{U}) = \Gamma_{(3,2)}^{(1,0)}(\mathcal{U}).$$

**Notation 4.1.** We denote by  $\mathcal{M}[m, n]$  the set of all global mosaic patterns that have parameters  $(z, a) \in [m, n]$ .

**Theorem 4.2.** *Let  $a\varepsilon > 0$ ,  $m, n \in [0, 1, 2, 3, 4]$ , and let  $\alpha = \max\{m, n\}$  and  $\beta = \min\{m, n\}$ . Then (1) exhibits spatial chaos if and only if  $\alpha \geq 2$  and  $\beta \geq 2$ .*

*Proof.* From Theorem 3.1, it is clear that  $\mathcal{M}[m, n]$  is increasing with respect to  $m$  and  $n$ . That is if  $m_1 \leq m_2$  and  $n_1 \leq n_2$ , then

$$\mathcal{M}[m_1, n_1] \subseteq \mathcal{M}[m_2, n_2].$$

To prove the theorem, it suffices to show that

$$h(\mathcal{M}[4, 1]) = h(\mathcal{M}[1, 4]) = 0 \quad (17)$$

and

$$h(\mathcal{M}[2, 2]) > 0. \quad (18)$$

We first prove (17). For  $a\varepsilon > 0$ ,  $(z, a) \in [4, 1]$  or  $[1, 4]$ , the only two global mosaic patterns are either all +’s or all -’s. Hence  $h(\mathcal{M}[4, 1]) = h(\mathcal{M}[1, 4]) = 0$ . To prove (18), we consider a global mosaic pattern that is an alternative array of vertical stripes of width 3 that are alternating in signs. See Fig. 4.

We shall assume the lower left corners of the  $3 \times 2$  rectangles that are boxed and are even. Restricting our observation to the  $9 \times 12$  rectangle containing those boxed rectangles, we conclude that each of the boxed rectangles can either remain the

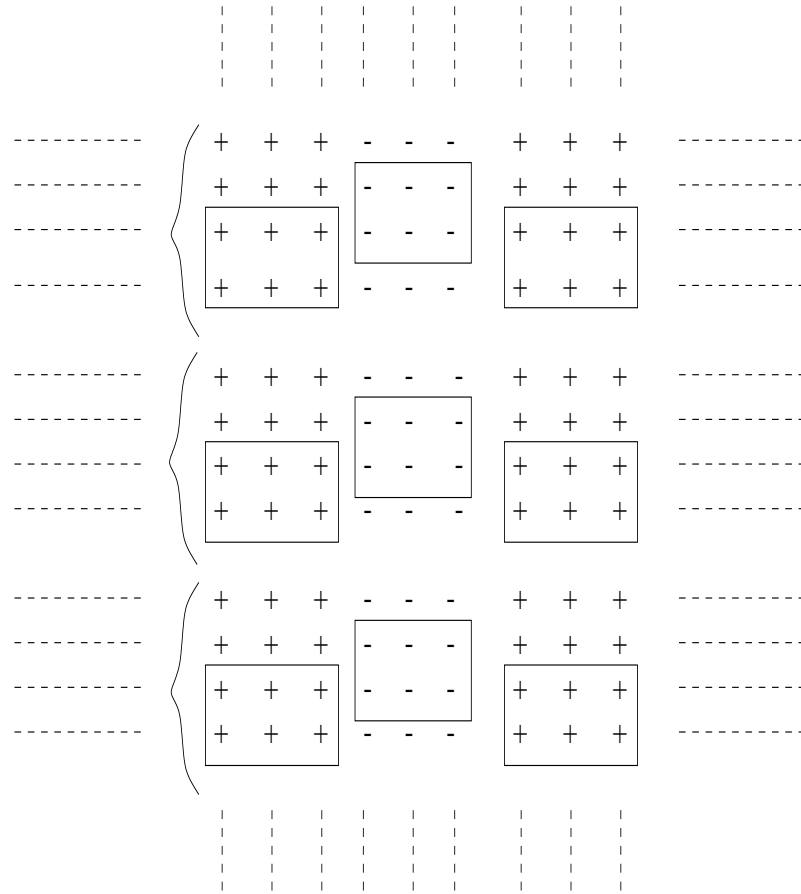


Fig. 4. Using Theorem 3.1 to find a lower bound for the spatial entropy of  $\mathcal{M}[2, 2]$  with  $a\varepsilon < 0$ .

same or be replaced by a rectangle of the same size that is filled with opposite signs. Thus, we see in general that for  $(i, j) \in \mathbb{Z}_E^2$

$$\Gamma_N^{(i,j)}(\mathcal{M}[2, 2]) \geq 2^{n^2},$$

where  $N = (3n, 4n)$ . Hence,

$$h_N^{(i,j)}(\mathcal{M}[2, 2]) \geq \frac{\log 2}{12}.$$

Using Theorem 4.1, we conclude that  $h(\mathcal{M}[2, 2]) \geq \log 2/12$ . ■

**Theorem 4.3.** *Let  $a\varepsilon < 0$ ,  $m, n \in \{1, 2, 3, 4\}$ . Then (1) exhibits spatial chaos if and only if  $m + n \geq 4$ .*

*Proof.* We only illustrate that

$$h(\mathcal{M}[2, 2]) > 0, \tag{19}$$

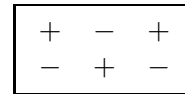
$$h(\mathcal{M}[1, 3]) = h(\mathcal{M}[3, 1]) > 0, \tag{20}$$

and

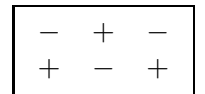
$$h(\mathcal{M}[2, 1]) = h(\mathcal{M}[1, 2]) = 0. \tag{21}$$

The other possibilities can be similarly treated as in Theorem 4.2.

Let  $a\varepsilon < 0$ ,  $(z, a) \in \mathcal{M}[2, 2]$ , so any + must have among its three interacting neighbors at least two -'s and any - must have among its three interacting neighbors at least two +'s. Consider the boxed  $3 \times 2$  rectangles



and



As offset in the figure below, any arrangement consisting solely of these  $3 \times 2$  rectangles whose lower left corners are even, i.e. are in  $\mathbb{Z}_E^2$ , makes a global mosaic pattern in  $\mathcal{M}[2, 2]$ . So, in every window of



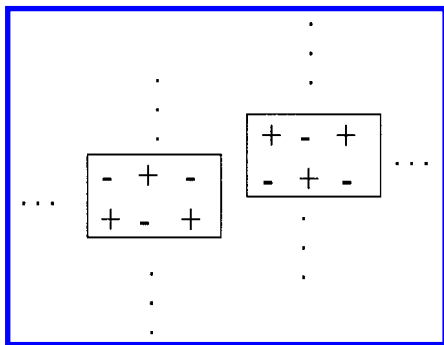


Fig. 5. Using Theorem 3.1 to find a lower bound for the spatial entropy of  $\mathcal{M}[2, 2]$  with  $a\varepsilon < 0$ .

size  $3n \times 2(n+1)$ , there are at least  $2^{n^2}$  distinct patterns. It follows that  $h(\mathcal{M}[2, 2]) \geq \log 2/6$ , giving (19).

Let  $a\varepsilon < 0$ ,  $(z, a) \in \mathcal{M}[1, 3]$ , so any  $+$  must have all three of its interacting neighbors as  $-$ 's and that any  $-$  must have among its three interacting neighbors at least one  $+$ . Define a  $3 \times 3$  rectangle

$$3 := \begin{matrix} - & - & + \\ - & + & - \\ + & - & - \end{matrix}$$

Consider the  $12 \times 12$  rectangles

$$1 := \begin{matrix} 3 & 3 & 3 & 3 \\ 3 & 3 & 3 & 3 \\ 3 & 3 & 3 & 3 \\ 3 & 3 & 3 & 3 \end{matrix}$$

and

$$2 := \begin{matrix} - & - & + & - & - & + & - & - & + & - & - & + \\ - & + & - & - & + & - & - & + & - & - & + & - \\ + & - & - & + & - & - & + & - & - & + & - & - \\ - & - & + & - & + & - & - & - & + & - & - & + \\ - & + & - & + & - & + & - & + & - & - & + & - \\ + & - & - & + & - & + & - & + & - & + & - & - \\ - & - & + & - & - & + & - & - & + & - & - & + \\ - & + & - & - & + & - & - & + & - & - & + & - \\ + & - & - & + & - & - & + & - & - & + & - & - \end{matrix}$$

Noting that both rectangles 1 and 2 are of the form

$$\begin{matrix} 3 & 3 & 3 & 3 \\ 3 & & & 3 \\ 3 & & & 3 \\ 3 & 3 & 3 & 3 \end{matrix}$$

for some interior choices of  $6 \times 6$  rectangles, one can check that any arrangement consisting solely of rectangles 1 and 2 whose lower left corners are even, i.e. are in  $\mathbb{Z}_E^2$ , makes a global mosaic pattern in  $\mathcal{M}[1, 3]$ . So, in some window of size  $12n \times 12n$ , there are  $2^{n^2}$  distinct patterns. It follows that  $h(\mathcal{M}[1, 3]) \geq \log 2/144$ , giving (20).

As for (21), let  $a\varepsilon < 0$ ,  $(z, a) \in \mathcal{M}[1, 2]$ , so  $m = 1$  implies that any  $+$  must have all three of its interacting neighbors as  $-$ 's, and  $n = 2$  implies that any  $-$  must have among its three interacting neighbors at least two  $+$ 's. The latter implies that there

cannot be three horizontally consecutive  $-$ 's. So, the only global mosaic patterns which are possible are (a) the single "checkerboard" pattern of alternating  $+$ 's and  $-$ 's, and (b) those patterns which have somewhere two horizontally consecutive  $-$ 's. In case (b), one can see by tedious logical implications that the pattern must have two adjacent diagonal "stripes" of all  $-$ 's surrounded by alternating diagonal stripes of all  $+$ 's or all  $-$ 's. So, for all windows  $N$  which are  $N_1 \times N_2$ ,

$$\Gamma_N(\mathcal{U}) \leq 2 + 2 \max\{2 + N_1, 2 + N_2\}.$$

Inequality (21) follows. ■

We conclude by mentioning possible future related work. First, the classification of the defect patterns is of interest. It is numerically reported in

[Yeh, 1998] that CNNs with space-dependent template such as (4) can generate temporal chaos. The rigorous study of such phenomenon is of considerable interest. The other dynamics properties, such as stability, traveling waves and scrolling waves of CNNs addressed in this paper have not been addressed yet. Finally, in practice CNNs are implemented on a finite lattice. Thus, it is also desirable to study the dynamics of such CNNs on a finite lattice. In particular, how do the boundary conditions on finite lattice influence the dynamics properties and pattern formation of CNNs on infinite lattice (see e.g. [Shih, 2000]).

## Acknowledgment

We thank Dr. C. J. Yu for providing the simulation work in the paper.

## References

- Chow, S. N. & Mallet-Paret, J. [1995a] "Pattern formation and spatial chaos in lattice dynamical system, I," *I. IEEE Trans. Circuits Syst.* **42**, 746–751.
- Chow, S. N. & Mallet-Paret, J. [1995b] "Pattern formation and spatial chaos in lattice dynamical systems, II," *IEEE Trans. Circuits Syst.* **42**, 752–756.
- Chow, S. N., Mallet-Paret, J. & Van Vleck, E. S. [1996a] "Pattern formation and spatial chaos in spatially discrete evolution equations," *Rand. Comput. Dyn.* **4**(2 & 3), 109–178.
- Chow, S. N., Mallet-Paret, J. & Van Vleck, E. S. [1996b] "Dynamics of lattice differential equations," *Int. J. Bifurcation and Chaos* **9**, 1605–1621.
- Chua, L. O. & Yang, L. [1988a] "Cellular neural networks: Theory," *IEEE Trans. Circuits Syst.* **35**, 1257–1272.
- Chua, L. O. & Yang, L. [1988b] "Cellular neural networks: Applications," *IEEE Trans. Circuits Syst.* **35**, 1273–1290.
- Chua, L. O. & Roska, T. [1993] "The CNN paradigm," *IEEE Trans. Circuits Syst.* **40**, 147–156.
- Chua, L. O. [1998] *CNN: A Paradigm for Complexity*, World Scientific Series on Nonlinear Science, Series A, Vol. 31 (World Scientific, Singapore).
- Crounse, K. R., Chua, L. O., Thiran, P. & Setti, G. [1996] "Characterization and dynamics of pattern formation in cellular neural networks," *Int. J. Bifurcation and Chaos* **6**, 1703–1724.
- Hsu, C. H., Juang, J., Lin, S. S. & Lin, W. W. [2000] "Cellular neural networks: Local patterns for general templates," *Int. J. Bifurcation and Chaos* **7**, 1645–1659.
- Juang, J. & Lin, S. S. [1997] "Cellular neural networks: Defect pattern and spatial chaos," preprint.
- Juang, J. & Lin, S. S. [2000] "Cellular neural networks: Mosaic pattern and spatial chaos," *SIAM J. Appl. Math.* **60**, 891–915.
- Shih, C. W. [1998] "Pattern formation and spatial chaos for cellular neural networks with asymmetric templates," *Int. J. Bifurcation and Chaos* **8**, 1907–1936.
- Shih, C. W. [2000] "Influence of boundary conditions on pattern formation and spatial chaos," *SIAM J. Appl. Math.* **61**(1), 335–368.
- Special Issue [1995] "Nonlinear waves, patterns and spatio-temporal chaos in dynamic arrays," *IEEE Trans. Circuits Syst. I* **42**(10).
- Thiran, P., Crounse, K. R., Chua, P. O. & Hasler, M. [1995] "Pattern formation properties of autonomous cellular neural networks," *IEEE Trans. Circuits Syst.* **42**, 757–774.
- Thiran, P. [1997] *Dynamics of Self-Organization of Locally Coupled Neural Networks*, Presses Polytechniques et Universitaires Romandes, Lausanne.
- Yen, L. C. [1998] *Cellular Neural Networks: Templates and Temporal Chaos*, Thesis, National Chiao Tung University, Taiwan.
- Zou, F. & Nossek, J. A. [1991] "A chaotic attractor with cellular neural networks," *IEEE Trans. Circuits Syst.* **38**, 811–812.
- Zou, F. & Nossek, J. A. [1992] "Cellular neural networks and the double scroll," *Proc. ISCAS'92*, San Diego, 1, pp. 320–323.
- Zou, F., Katérle, A. & Nossek, J. A. [1993] "Homoclinic and heteroclinic orbits of the three-cell cellular neural networks," *IEEE Trans. Circuits Syst.* **40**, 843–844.
- Zou, F. & Nossek, J. A. [1993] "Bifurcation and chaos in cellular neural networks," *IEEE Trans. Circuits Syst.* **40**, 166–173.

## Appendix

The purpose of the simulations is to support the assertions of Theorem 2.1(ii) and Theorem 3.1. In the following figures, all the lower-left  $1 \times 1$  boxes are assumed to be at the integer lattice  $(0, 0)$ . If the output  $f(x_{i,j})$  of the state of a cell  $C_{i,j}$  is  $+1$  (resp.  $-1$ ), then we use black (resp. white) to color its associated box. Numerical tables give values of the states  $x_{i,j}$ .

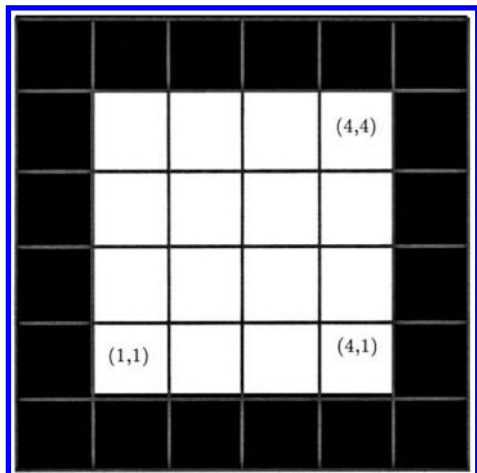
In Fig. 6, we pick  $\varepsilon = 1/6$  and  $(z, a) \in [3, 2]$  region. According to Theorem 3.1, in Fig. 6(c), the outputs of the cells at  $(4, 4)$  and  $(4, 1)$  are initially white but cannot remain white. The basic mosaic patterns whose centers are at  $(i, j)$ ,  $0 \leq i, j \leq 5$ ,  $(i, j) \neq (4, 4)$ ,  $(i, j) \neq (4, 1)$  are initially good.

1.5	1.5	1.5	1.5	1.5	1.5
1.5	-1.5	-10	-10	-10	1.5
1.5	-7	-5	-10	-1.5	1.5
2.5	-1.5	-8	-1.5	-5	1.5
1.5	-1.5	-2.5	-1.5	-1.5	1.5
1.5	1.5	1.5	1.5	1.5	1.5

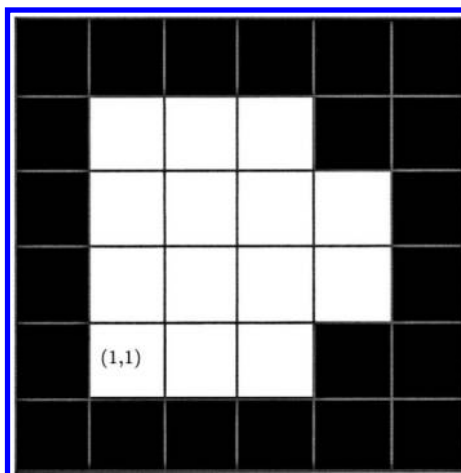
(a)

1.9	1.9	1.5	1.9	1.9	1.9
1.5	-1.3	-1.3	-1.3	1.5	1.9
1.5	-1.3	-1.7	-1.7	-1.3	1.5
1.5	-1.3	-1.7	-1.7	-1.3	1.5
1.5	-1.3	-1.3	-1.3	1.5	1.9
1.9	1.9	1.5	1.9	1.9	1.9

(b)



(c)



(d)

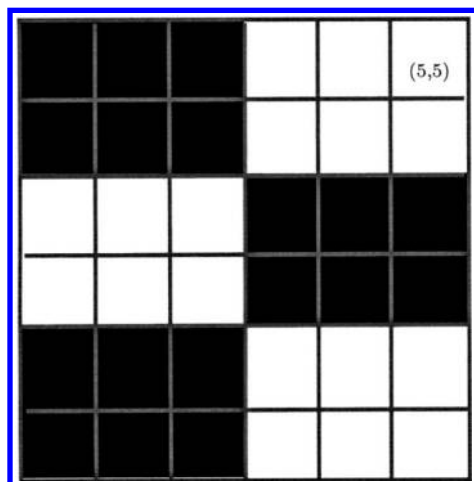
Fig. 6. [3, 2] region:  $a = 1.2$ ,  $\varepsilon = 1/6$ ,  $z = 0.1$ .

1.5	1.5	1.5	-1.5	-1.5	-1.5
1.5	1.5	1.5	-2	-2	-2
-1.5	-1.5	-1.5	1.5	1.5	1.5
-1.5	-1.5	-1.5	1.5	1.5	1.5
1.5	1.5	1.5	-1.5	-1.5	-1.5
1.5	1.5	1.5	-1.5	-1.5	-1.5

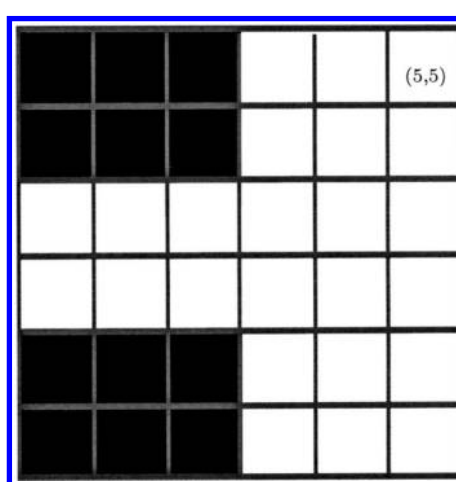
(a)

1.167	1.5	1.167	-1.167	-1.5	-1.167
1.167	1.167	1.167	-1.167	-1.5	-1.167
-1.5	-1.167	-1.5	-1.5	-1.5	-1.5
-1.5	-1.167	-1.5	-1.5	-1.5	-1.5
1.167	1.167	1.167	-1.167	-1.5	-1.167
1.167	1.5	1.167	-1.167	-1.5	-1.167

(b)



(c)



(d)

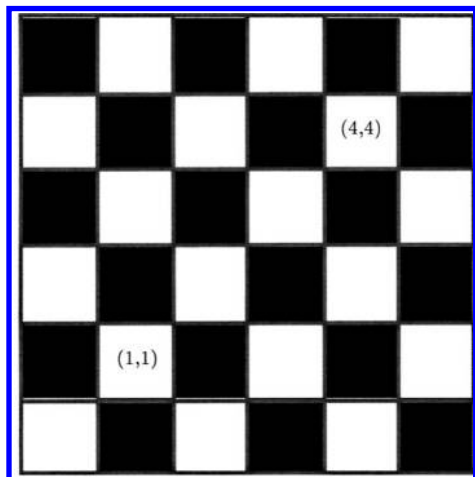
Fig. 7. [2, 2] region:  $a = 1$ ,  $\varepsilon = 1/6$ ,  $z = 0$ .

1.5	-1.5	1.5	-1.5	1.5	-1.5
-1.5	1.5	-1.5	2.5	-1.5	1.5
1.5	-2.5	1.5	-1.5	1.5	-1.5
-2.5	1.5	-1.5	1.5	-1.5	1.5
1.5	-1.5	2.5	-1.5	1.5	-1.5
-1.5	1.5	-1.5	1.5	-1.5	1.5

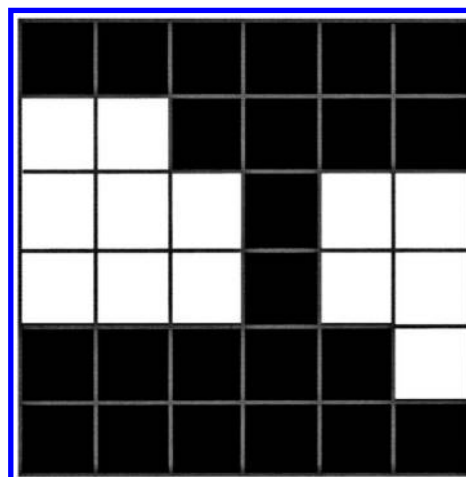
(a)

1.75	2.25	2.25	2.25	2.25	2.25
-1.25	-1.75	1.75	2.25	2.25	1.25
-2.25	-2.25	-1.75	1.25	-1.75	-1.75
-2.25	-1.75	-1.75	1.25	-1.75	-2.25
1.75	1.75	2.25	2.25	1.75	-1.25
2.25	2.25	2.25	2.25	2.25	2.25

(b)



(c)



(d)

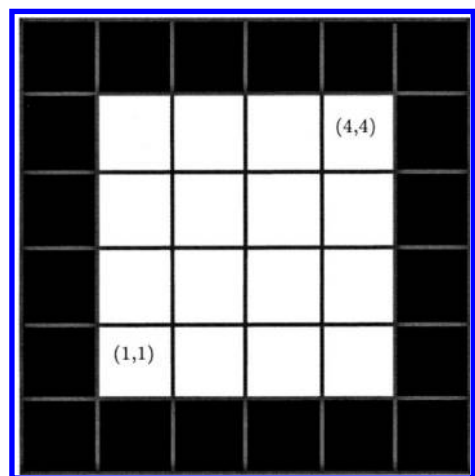
Fig. 8.  $[3, 3]$  region:  $a = 1.5$ ,  $\varepsilon = 1/6$ ,  $z = 0$ .

1.5	1.5	1.5	1.5	1.5	1.5
1.5	-1.5	-10	-10	-10	1.5
1.5	-7	-5	-10	-1.5	1.5
2.5	-1.5	-8	-1.5	-5	1.5
1.5	-1.5	-2.5	-1.5	-1.5	1.5
1.5	1.5	1.5	1.5	1.5	1.5

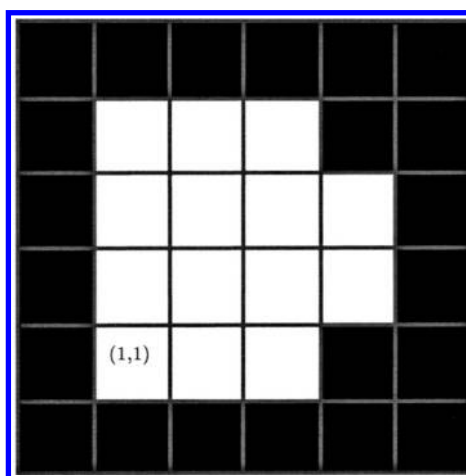
(a)

4	4	3.33	4	4	4
3.33	-1.33	-1.33	-1.33	3.33	4
3.33	-1.33	-2	-2	-1.33	3.33
3.33	-1.33	-2	-2	-1.33	3.33
3.33	-1.33	-1.33	-1.33	3.33	4
4	4	3.33	4	4	4

(b)



(c)



(d)

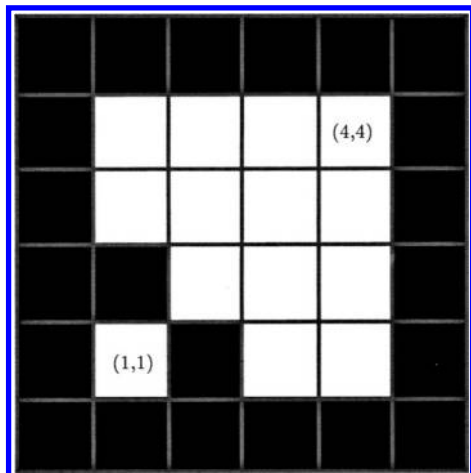
Fig. 9.  $[4, 2]$  region:  $a = 2$ ,  $\varepsilon = 1/6$ ,  $z = 1$ .

1.5	1.5	1.5	1.5	1.5	1.5
1.5	-1.5	-10	-10	-10	1.5
1.5	-7	-5	-10	-1.5	1.5
2.5	1.5	-8	-1.5	-5	1.5
1.5	-1.5	2.5	-1.5	-1.5	1.5
1.5	1.5	1.5	1.5	1.5	1.5

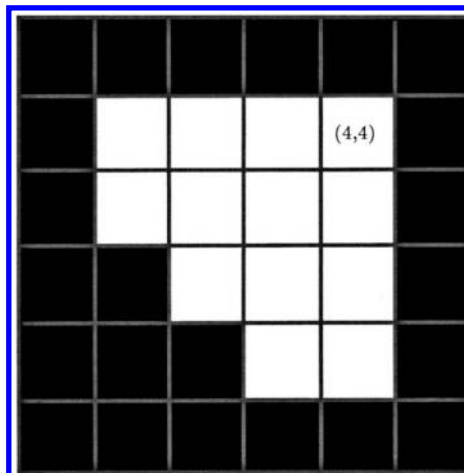
(a)

5.5	5.5	4.5	5.5	4.5	5.5
4.5	-2.5	-2.5	-3.5	-1.5	4.5
4.5	-2.5	-3.5	-3.5	-2.5	4.5
5.5	4.5	-2.5	-3.5	-2.5	4.5
5.5	5.5	4.5	-2.5	-1.5	4.5
5.5	5.5	5.5	5.5	4.5	5.5

(b)



(c)



(d)

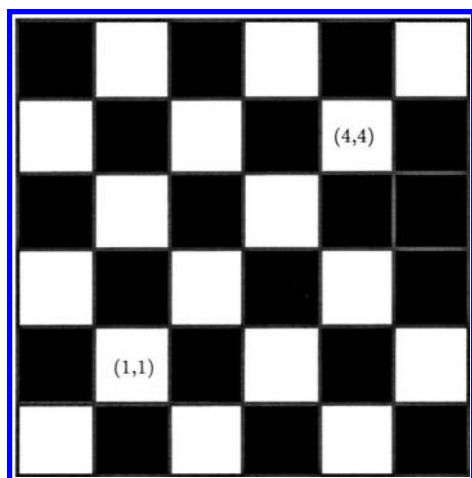
Fig. 10. [4, 3] region:  $a = 2$ ,  $\varepsilon = 1/6$ ,  $\varepsilon = 1/6$ ,  $z = 1$ .

1.5	-1.5	1.5	-1.5	1.5	-1.54
-1.5	1.5	-1.5	4.5	-1.5	1.5
1.5	-2.5	1.5	-1.5	1.5	1.5
-2.5	1.5	-1.5	1.5	-1.5	1.5
1.5	-1.5	2.5	-1.5	1.5	-1.5
-1.5	1.5	-1.5	1.5	-1.5	1.5

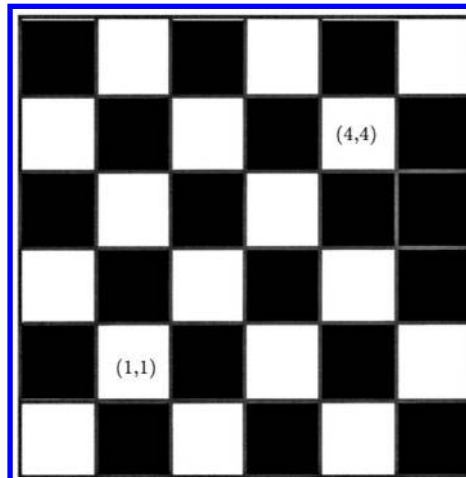
(a)

1.5	-1.5	1.5	-1.5	1.5	-1.5
-1.5	1.5	-1.5	1.5	-1.5	2.5
2.5	-1.5	1.5	-1.5	2.5	4.5
-1.5	1.5	-1.5	1.5	-1.5	1.5
1.5	-1.5	1.5	-1.5	1.5	-1.5
-1.5	1.5	-1.5	1.5	-1.5	1.5

(b)



(c)



(d)

Fig. 11. [4, 4] region:  $a = 3$ ,  $\varepsilon = 1/6$ ,  $z = 1$ .

Therefore, in Fig. 6(d) the final outputs seem to be very reasonable. Note also that the evolution from the unstable pattern in Fig. 6(c) to the pattern in Fig. 6(d) involves the least number of changes to arrive at a final, stable pattern.

Indeed, we see that all figures of evolution from unstable to stable patterns, for parameters  $(z, a, \varepsilon)$  corresponding to the  $[3, 2]$ ,  $[2, 2]$ ,  $[3, 3]$ ,  $[4, 2]$ ,  $[4, 3]$  and  $[4, 4]$  regions, are consistent with the theory proved in Theorem 2.1(ii) and Theorem 3.1.

**This article has been cited by:**

1. JONQJUANG, SHIH-FENG SHIEH. 2004. ON THE SPATIAL ENTROPY OF TWO-DIMENSIONAL GOLDEN MEAN. *International Journal of Bifurcation and Chaos* 14:01, 309-319. [[Abstract](#)] [[References](#)] [[PDF](#)] [[PDF Plus](#)]